LA-UR-97-1905

Title:

The Effect of the New Nucleon-Nucleus Elastic Scattering Data in LAHET™ Version 2.8 on Neutron Displacement Cross Section Calculations

Author(s): E. J. Pitcher, P. D. Ferguson, G. J. Russell, R. E. Prael, D. G. Madland, J. D. Court and L. L. Daemen

Submitted to:

http://lib-www.lanl.gov/la-pubs/00347911.pdf

Los Alamos
NATIONAL LABORATORY

The Effect of the New Nucleon-Nucleus Elastic Scattering Data in LAHET™ Version 2.8 on Neutron Displacement Cross Section Calculations

E. J. Pitcher, P. D. Ferguson, G. J. Russell, R. E. Prael, D. G. Madland, J. D. Court and L. L. Daemen
Los Alamos National Laboratory
Los Alamos, NM 87545

M. S. Wechsler
North Carolina State University
Raleigh, NC 27695

Abstract

The latest release of the medium-energy Monte Carlo transport code LAHET [1] includes a new nucleon-nucleus elastic scattering treatment based on a global medium-energy phenomenological optical-model potential. Implementation of this new model in LAHET allows nuclear elastic scattering for neutrons with energies greater than 15 MeV and for protons with energies greater than 50 MeV. Previous investigations on the impact of the new elastic scattering data revealed that the addition of the proton elastic scattering channel can lead to a significant increase in the calculated damage energy under certain conditions.

We report here results on the impact of the new elastic scattering data on calculated displacement cross sections in various elements for neutrons with energies in the range 16 to 3160 MeV. Calculated displacement cross sections at 20 MeV in low-mass materials are in better agreement with SPECTER-calculated cross sections.

Introduction

The capability to treat neutron elastic scattering has always existed in LAHET. In early versions, the user could provide tabulated elastic scattering cross section data and elastic scattering would be included in neutron transport. With later versions, a default set of elastic scattering data was provided with LAHET (i.e., the ELSTIN file). These data were generated with the SCAT79 optical model code using the Becchetti-Greenlees potential [2], which is generally considered to be accurate up to about 50 MeV. With version 2.70, elastic cross section data are provided for 98 isotopes, tabulated on a 17-point energy grid from 20 to 100 MeV (the LELSTIN file). Beyond 100 MeV, elastic scattering is ignored in LAHET2.70.

Recently, new nucleon-nucleus elastic scattering data have been incorporated into the latest release, LAHET version 2.8 [3]. In the energy range 50 to 400 MeV, these tabulated cross sections were generated with a global medium-energy nucleon-nucleus phenomenological optical-model potential. Comparison of model predictions to experimental data shows generally good agreement [4]. For neutron and proton energies above 400 MeV and for neutron energies below 50 MeV, tabulations generated from the HERMES code [5] are used. Further details on the development of the nucleon-nucleus optical-model potential from which the elastic scattering data are derived are given in [3,4,6,7].

Another recently-added feature of the LAHET Code System is the capability to tally recoil energy and damage energy spectra with the postprocessing code HTAPE. The damage energy is obtained from the recoil energy using a parameterization due to Robinson [8] of the Lindhard function [9,10], which partitions the recoil energy into nuclear and electronic components. The tally calculates the total damage energy and its elastic component. This capability has been used extensively to calculate damage parameters for materials irradiated in spallation neutron source environments [11,12,13,14,15].

One characteristic of the LAHET-calculated neutron displacement cross section is that it consistently underpredicts the value at 20 MeV calculated using the radiation damage code SPECTER [16]. This has been observed for the following targets: Li, Be, C, Al, Al-6061, Fe, 316 stainless steel [11,14], Inconel-718 [14], Cu [15], and W [13-15]. SPECTER uses evaluated nuclear data in estimating damage energy and so is generally considered to be more accurate than LAHET. The prime motivation for incorporating the refined elastic scattering data in LAHET2.8 was to improve LAHET's ability to accurately calculate damage parameters at low energy. We show here that, for low-mass materials, agreement between SPECTER and LAHET at 20 MeV is much improved with the new elastic scattering data. For medium-mass materials, the displacement cross section at low energies is slightly lower, but is higher by ~20% beyond 50 MeV. And for high-mass materials, the displacement cross section is largely unaffected by the new elastic scattering model. Schubin et al. [17] have reported displacement cross section calculations using DISCA + SCAT2 that are in good agreement with SPECTER at 20 MeV, but no details were given concerning the codes employed.

Calculational Method

The method for calculating the damage energy cross section and, from it, the displacement cross section is described in [13]. We use this same technique here. We model a 1-cm-thick slab of material with a normalized density of 0.01 atoms/b·cm, and launch a pencil beam of neutrons onto the slab. A typical LAHET input deck (for 100-MeV neutrons on Fe) used in these calculations is shown in Table I. Default physics model settings are used except for the following items (see [1] for item descriptions): NBERTP = –1, NSPRED = –5, ICPT = 1, and ELAS = 100. Since we are dealing with essentially a thin target, only the last item influences results reported here. Setting ELAS = 100 simply extends the elastic scattering treatment from 50 to 100 MeV when running LAHET2.70. In addition one other parameter is changed for LAHET2.82 input decks: the low energy cutoff for neutrons is changed from the default value of 20 MeV to 15 MeV by setting ELON = 15, which allows us to calculate the displacement cross section down to 15 MeV with LAHET2.82.

Using the damage energy tally in HTAPE (IOPT=16), we analyze the history tape written by LAHET and calculate the mean damage energy per source neutron T_{dam} both the total and its elastic component. The

Table I. Typical LAHET2.82 input deck (100-MeV neutrons on iron).

```
radiation damage in iron
pencil neutron beam incident on a 1-cm slab

3000000,1,1,98,800000,33000000,,,,,1/
-1,,0,,,1/
1,0,1,1,1,0,1,1/
18*0/
-5,,,,,,,1/
,,15,,,,100/
0.00000E+00, 4, 4/
26,54,0.000590,43/26,56,0.009172,44/26,57,0.000210,45/
26,58,0.000028,46/
1     1   1    1  -2  -3
2     0       -4  #1
999   0        4

  1   pz    0.0
  2   pz    1.0
  3   cz    1.0
  4   so   10.0

in   1 1 0

0, 100.0000,1,0.000001,0/
```

damage energy cross section σ_e is then given by $\sigma_e = T_{dam}/N_v x$, where N_v is the atom density and x is the target thickness ($N_v x = 0.01$ b^{-1} for all calculations reported here). The displacement cross section σ_d is calculated from $\sigma_d = (\beta/2T_d)\sigma_e$, where T_d is the threshold displacement energy, and $\beta = 0.8$ is intended to compensate for forward scattering in the displacement cascade while the factor 2 in the denominator accounts for energy lost to subthreshold reactions [10]. We investigated 15 different elements, which are listed in Table II. Also listed in Table II is the assumed T_d for each element, taken from [16], with the exception of tin whose value is assumed to be 60 eV. For LAHET2.70, the displacement cross section was calculated at 45 different energies ranging from 20.0 MeV to 3.16 GeV. Intermediate energies are 20 points per decade, equally spaced in lethargy. The same energy structure is used for LAHET2.82, with two additional energies at 15.8 and 17.8 MeV, which we add since the elastic scattering data in LAHET2.82 extend down to 15 MeV.

Each calculation used 3 million source neutrons, giving a one-standard-deviation statistical confidence interval less than 3% on the cross section value for all elements, and less than 1% for medium- and high-mass elements. Results are shown in Figures 1 through 15. Each figure has two curves, one showing the calculated results using LAHET version 2.70 (open circles, labeled 2.70), and the other curve representing LAHET version 2.82 (solid circles, labeled 2.82).

Table II. Elements for which neutron displacement cross sections have been calculated, and their assumed threshold displacement energies.

Element	T_d (eV)
lithium	10
beryllium	31
carbon	31
aluminum	27
silicon	25
chromium	40
iron	40
nickel	40
copper	40
zirconium	40
molybdenum	60
tin	60
tantalum	53
tungsten	90
lead	25

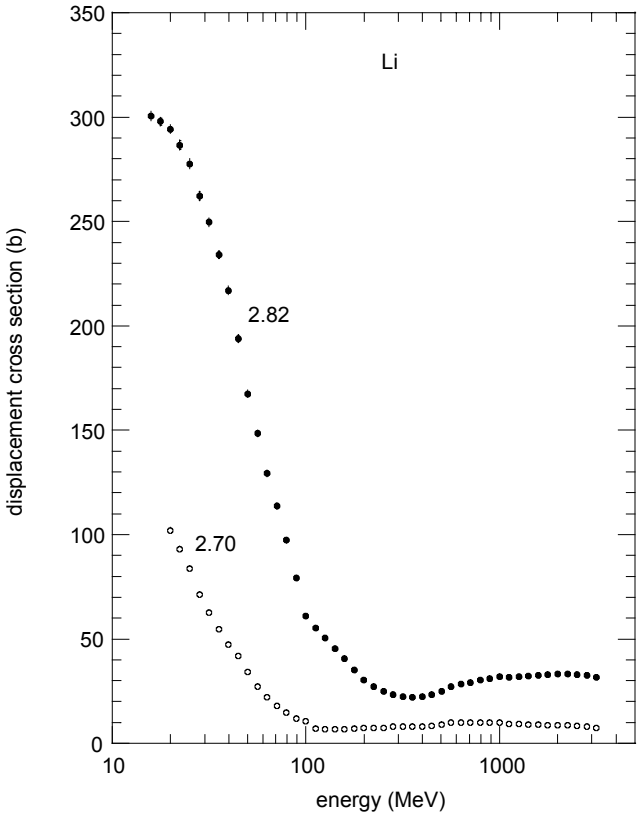

Figure 1. Calculated displacement cross section in lithium.

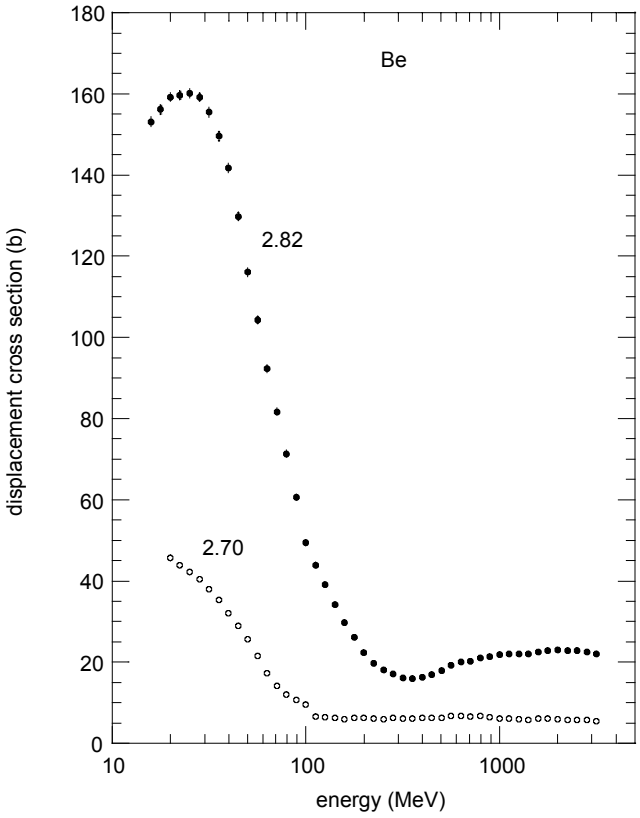

Figure 2. Calculated displacement cross section in beryllium.

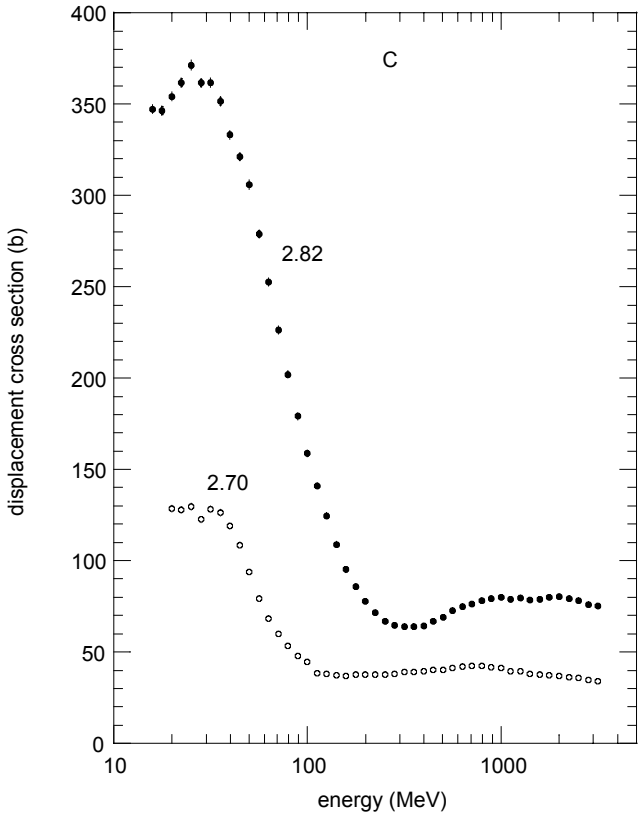

Figure 3. Calculated displacement cross section in carbon.

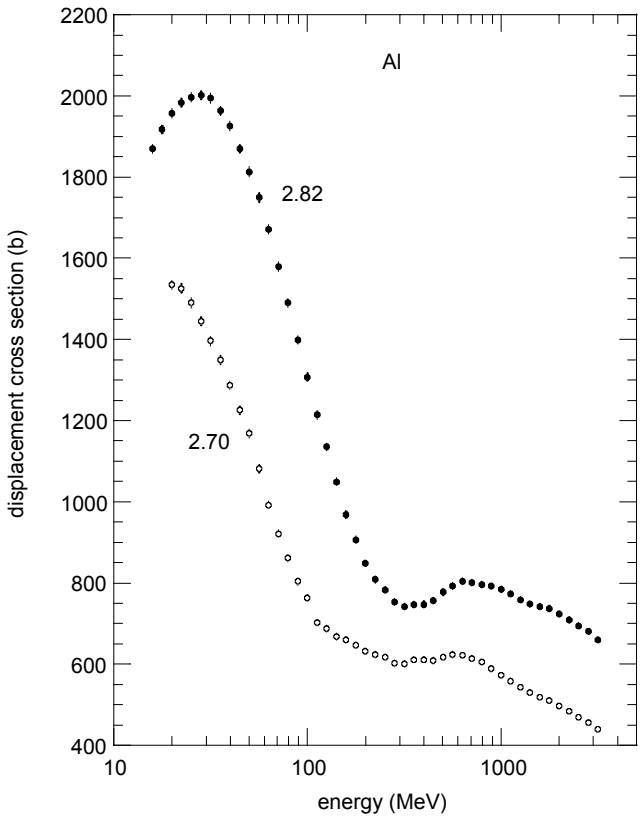

Figure 4. Calculated displacement cross section in aluminum.

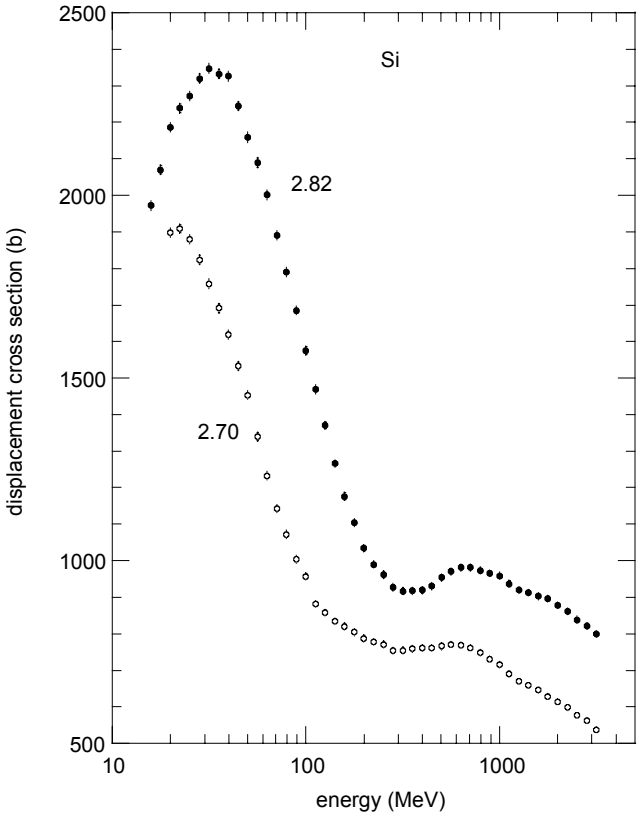

Figure 5. Calculated displacement cross section in silicon.

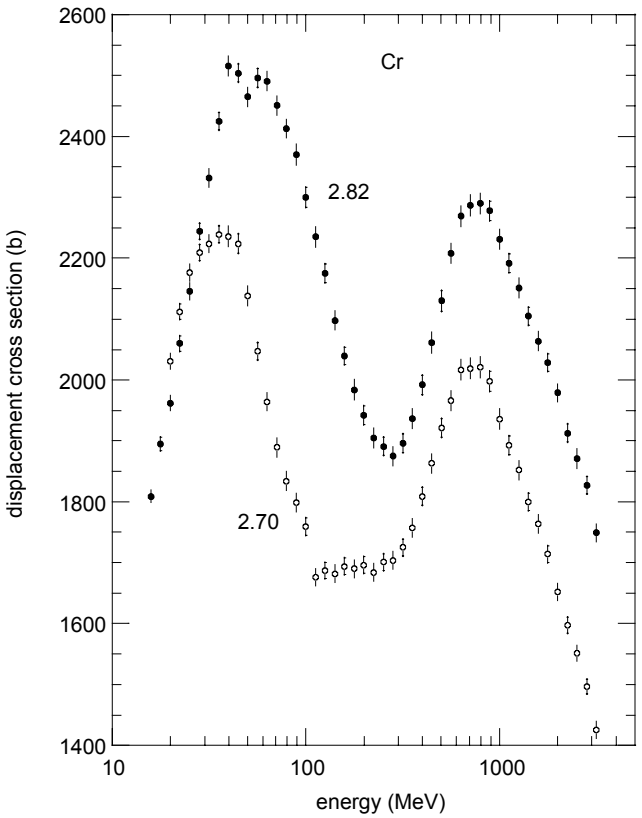

Figure 6. Calculated displacement cross section in chromium.

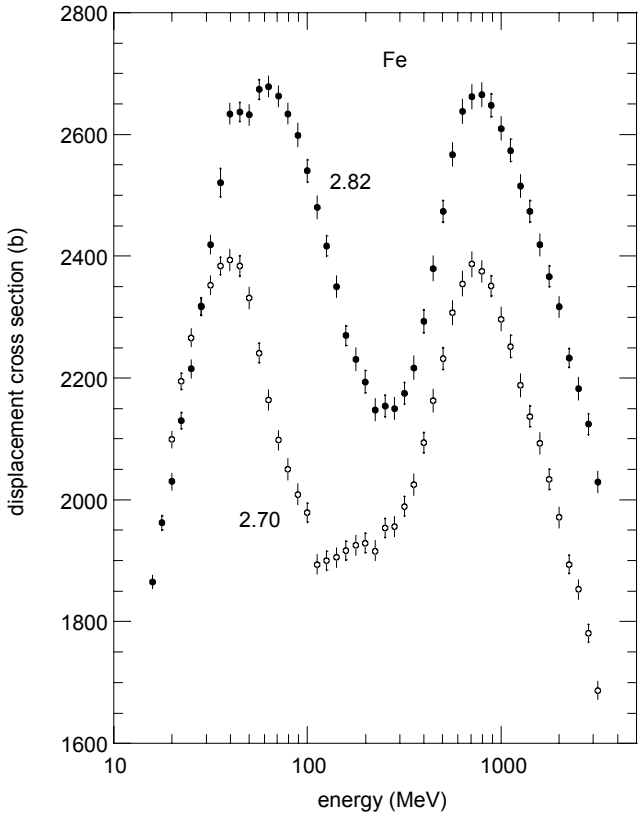

Figure 7. Calculated displacement cross section in iron.

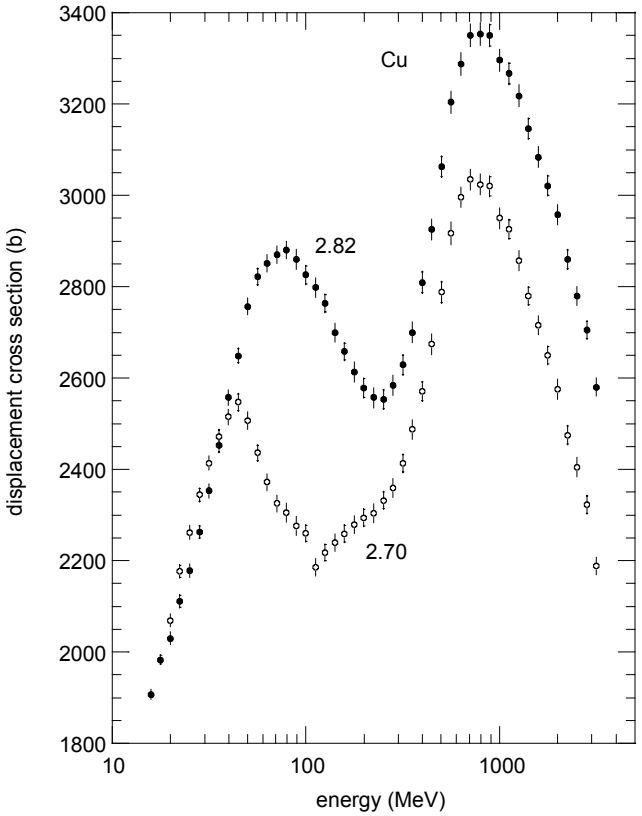

Figure 9. Calculated displacement cross section in copper.

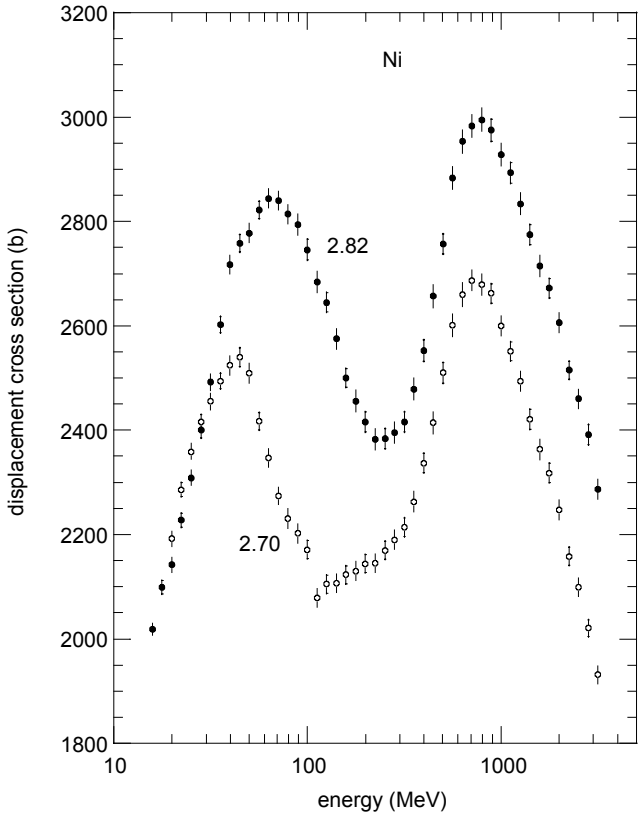

Figure 8. Calculated displacement cross section in nickel.

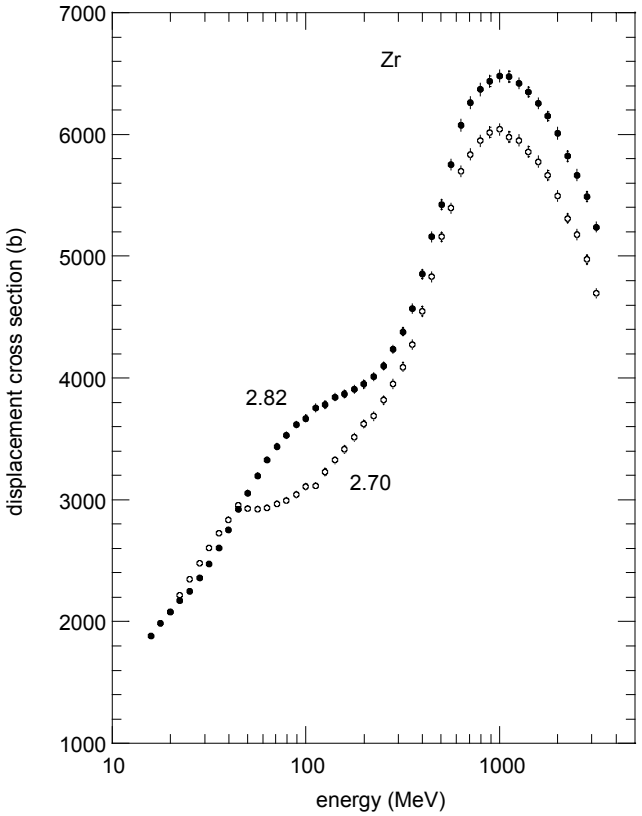

Figure 10. Calculated displacement cross section in zirconium.

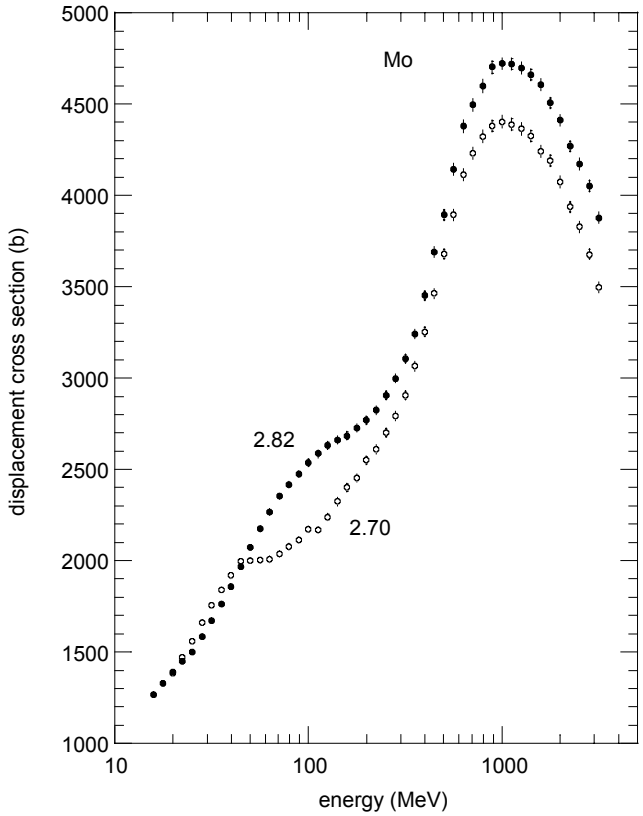

Figure 11. Calculated displacement cross section in molybdenum.

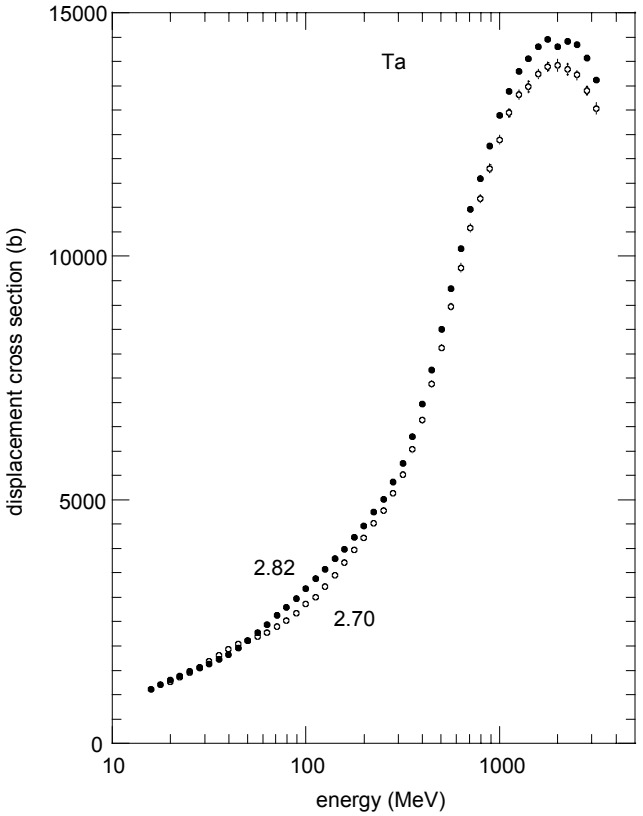

Figure 13. Calculated displacement cross section in tantalum.

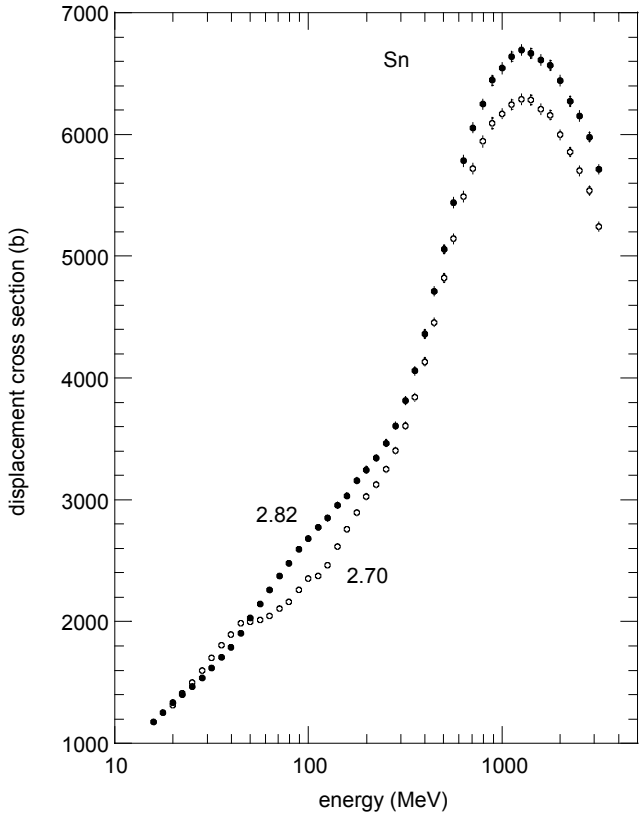

Figure 12. Calculated displacement cross section in tin.

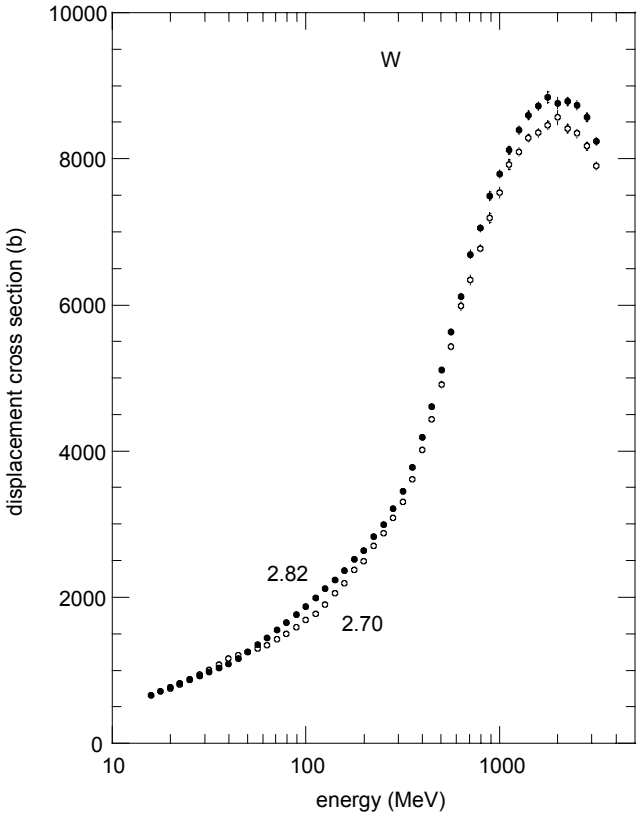

Figure 14. Calculated displacement cross section in tungsten.

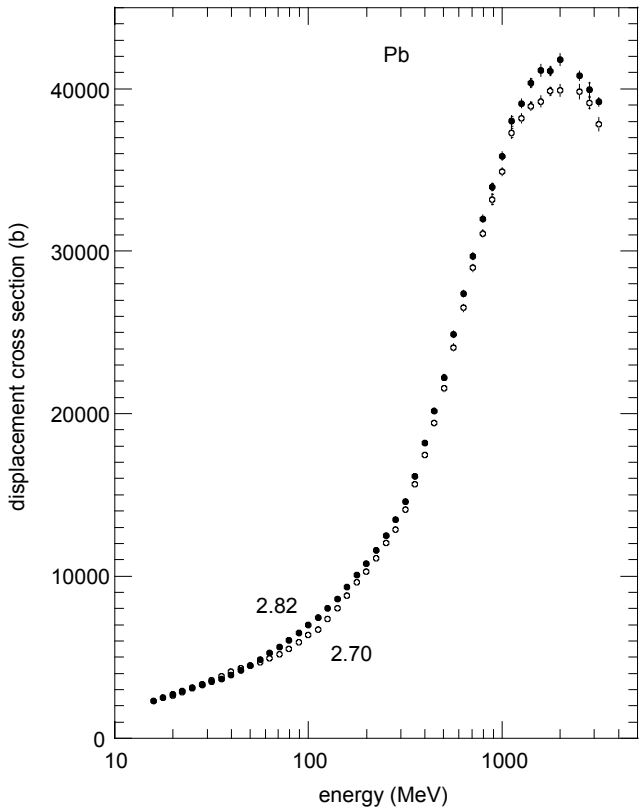

Figure 15. Calculated displacement cross section in lead.

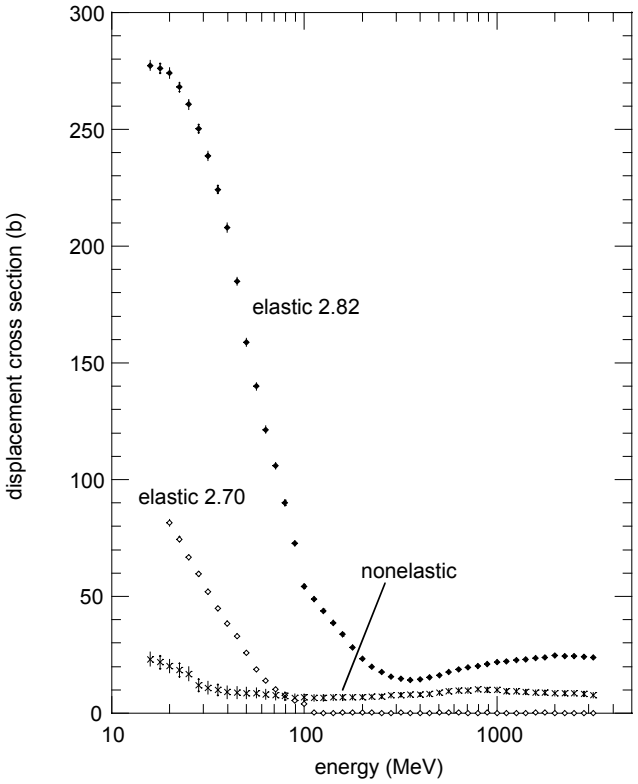

Figure 16. Elastic and nonelastic contributions to the displacement cross section in lithium.

Discussion of Results

The difference between the displacement cross sections calculated with LAHET versions 2.70 and 2.82 is substantial in low-mass materials, as seen in Figures 1 through 5. The difference is most prominent at low energies. Figure 16 shows the elastic contribution to the displacement cross section for versions 2.70 and 2.82, as well as the contribution from nonelastic reactions (identical for both versions) in lithium. Note that, at 20 MeV, the elastic component is nearly four times larger for version 2.82 as compared to 2.70. Further, nonelastic reactions account for only a small fraction of the total displacement cross section at this energy. Thus, the displacement cross section is higher by nearly a factor of three at 20 MeV. For version 2.70, the elastic component drops to zero beyond 100 MeV, whereas version 2.82 has an elastic contribution that is more than seven times greater than the nonelastic component at 100 MeV.

The difference between the two versions grows smaller as the target mass increases. This is due to the fact that nonelastic reactions account for an increasing fraction of the total displacement cross section with increasing mass. For medium-mass elements, the difference between the two versions does not vary by more than about 20%. Figure 17 shows the elastic and nonelastic components of the displacement cross section for nickel. Note the nonelastic component dominates at all energies. The medium-mass elements seen in Figures 6 through 9 exhibit two prominent peaks in the displacement cross section. Figure 17 shows that the low-energy peak is due to elastic reactions while the high-energy peak derives from nonelastic reactions. The elastic components in both versions agree with one another at energies below about 35 MeV. Beyond this energy the elastic components diverge and version 2.82 produces a total cross section that is consistently higher than that calculated by version 2.70.

In high-mass targets, represented in Figures 10 through 15, the elastic

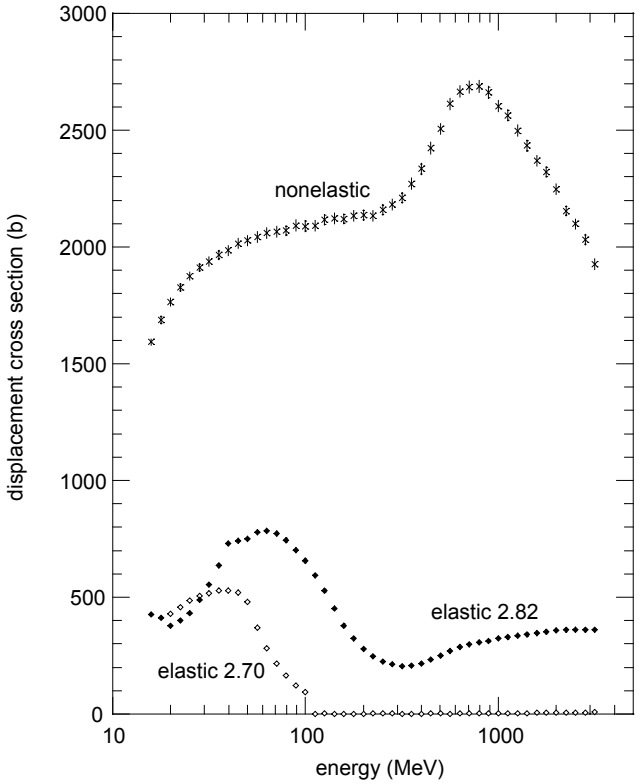

Figure 17. Elastic and nonelastic contributions to the displacement cross section in nickel.

contribution is small and we observe only small differences between the two versions, most notably in the energy region 50 to about 300 MeV. Beyond 100 MeV the elastic scattering channel is turned off in version 2.70, leading to the observed discrepancy. The elastic and nonelastic contributions to the displacement cross section for a typical high-mass element, tin, is shown in Figure 18.

As mentioned in the introduction, LAHET has historically underpredicted the neutron displacement cross section at 20 MeV when compared to results of the damage code SPECTER. SPECTER results are generally considered more reliable as they are derived from evaluated nuclear data, whereas LAHET is a model-based code whose applicability below about 150 MeV is questionable. Table III lists the displacement cross section values at 20 MeV derived from SPECTER and LAHET versions 2.70 and 2.82 for a selected set of elements. For low-mass nuclides, where the nonelastic contribution to the displacement cross section is small, version 2.82 is in better agreement with SPECTER, although the discrepancy is still appreciable. The new elastic scattering data make up approximately half of the difference observed between version 2.70 and SPECTER. This is shown graphically in Figure 19, where we plot the relative difference between SPECTER and LAHET as a function of the target atomic number. Note the discrepancy for low-mass elements drops from 80% to 40% when the new elastic scattering data are used.

At medium and high masses, where the elastic scattering channel is not so important relative to the nonelastic, observed differences between the two versions of LAHET are not significant, and yet the observed discrepancy between LAHET and SPECTER is still in the range 30 to 40%. While the source of this discrepancy is not known with certainty, it is quite likely due to an underprediction by LAHET of nonelastic processes at low energies. It is well known that the intranuclear cascade models used by LAHET are less reliable at low energies, particularly for low-mass nuclei.

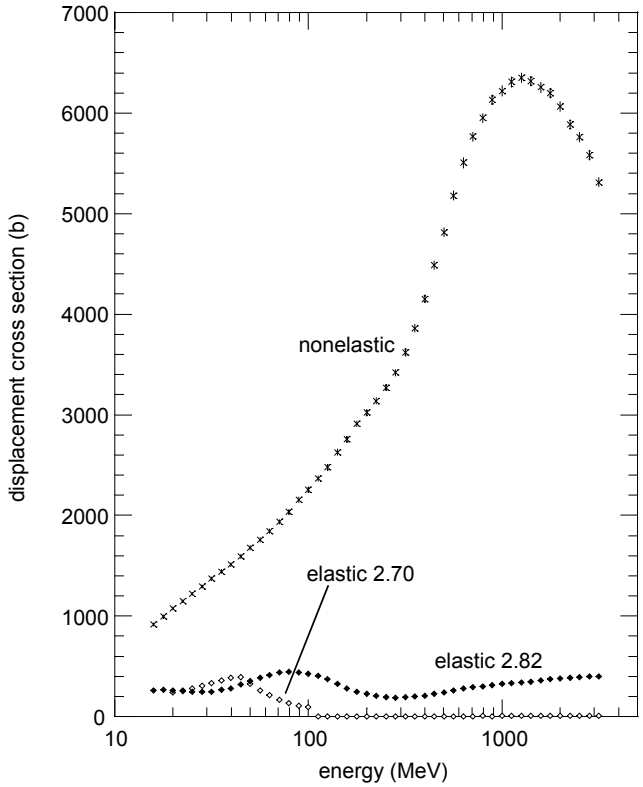

Figure 18. Elastic and nonelastic contributions to the displacement cross section in tin.

Table III. Comparison of calculated neutron displacement cross sections at 20 MeV, in units of barns.

Element	SPECTER	LAHET2.70	LAHET2.82
lithium	457.4	101.9	294.3
beryllium	275.5	45.7	159.2
carbon	578.4	128.4	354.2
aluminum	2660	1658	2114
iron	3078	2099	2030
tungsten	1188	750.2	769.3

Conclusions

Neutron displacement cross sections over the energy range near 20 to 3160 MeV have been calculated for 15 elements using LAHET versions 2.70 and 2.82. The new elastic scattering treatment incorporated in version 2.82 produces results at 20 MeV that are in better agreement with SPECTER-calculated cross sections. However, there is still a 30 to 40% discrepancy between LAHET and SPECTER over the entire range of target masses, most likely due to the use of LAHET below its range of applicability. An effort is currently underway at Los Alamos to extend evaluated nuclear data up to 150 MeV for a certain set of elements typically used in spallation source environments. Included in these new evaluations is a direct evaluation of the damage energy cross section. Beyond this energy, displacement cross sections calculated using LAHET should be reliable.

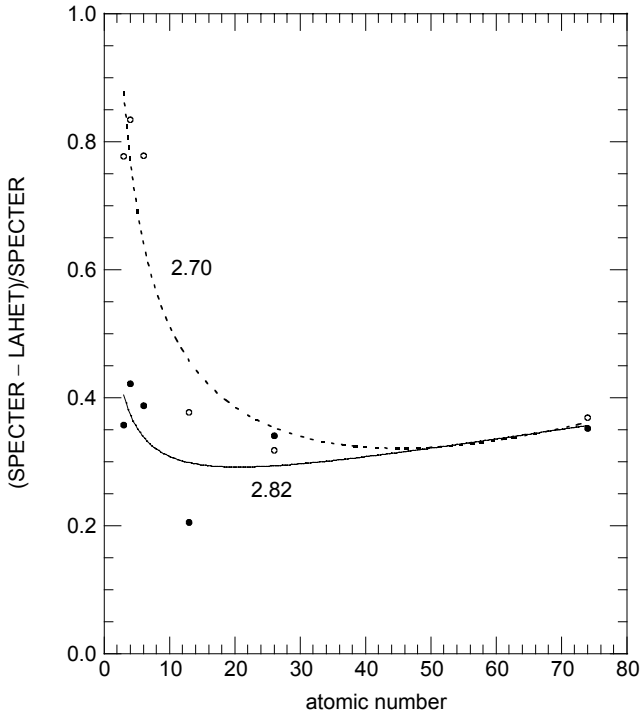

Figure 19. Relative discrepancy between SPECTER- and LAHET-calculated values of the neutron displacement cross section at 20 MeV as a function of atomic number. The open circles and dashed line are version 2.70 and the solid circles and solid line are version 2.82. The lines are guides to the eye.

References

1. R. E. Prael and H. Lichtenstein, "User Guide to LCS: The LAHET Code System" (Report LA-UR-89-3014, Los Alamos National Laboratory, 1989).

2. F. D. Becchetti and G. W. Greenlees, Phys. Rev. **182** (1969), 1190.

3. R. E. Prael and D. G. Madland, "LAHET Code System Modifications for LAHET2.8," (Report LA-UR-95-3605, Los Alamos National Laboratory, 1995).

4 D. G. Madland, "Recent Results in the Development of a Global Medium-Energy Nucleon-Nucleus Optical-Model Potential," *Proceedings of a Specialist's Meeting on Preequilibrium Reactions*, Semmering, Austria, February 10–12, 1988, B. Strohmaier, ed. (OECD, Paris, 1988), 103.

5. P. Cloth et al., "HERMES – A Monte Carlo Program System for Beam-Materials Interaction Studies" (Report Jul-2203, Kernforschungsanlage Julich GmbH, 1988).

6. R. E. Prael and D. G. Madland, "A nucleon-nucleus elastic scattering model for LAHET," *Proceeding of the 1996 Topical Meeting on Radiation Protection and Shielding*, No. Falmouth, Massachusetts (1996) 251.

7. D. G. Madland, "Progress in the Development of Global Medium-Energy Nucleon-Nucleus Optical Model Potentials," *Proceedings of the Specialists' Meeting on the Nucleon Optical Model up to 200 MeV*, Commissariat à l'Energie Atomique, Bruyères-le-Châtel, France, November 13-15, 1996, to be published by the OECD Nuclear Energy Agency, Paris.

8. M. T. Robinson, "The Dependence of Radiation Effects on the Primary Recoil Energy, pp. 397-429, in *Radiation-Induced Voids in Metals*, CONF-710601, U. S. Atomic Energy Commission, Washington, D. C., April 1972.

9. J. Lindhard, V. Nielson, and M. Scharff, "Approximation Method in Classical Screened Coulomb Fields," Notes on Atomic Collisions, I. Kongelige Danske Videnskabernes Selskab, Matematisk-Fysiske Meddeleiser, **36**, No. 10, Copenhagen, 1968.

10. Standard Practice for Neutron Radiation Damage Simulation by Charged-Particle Irradiation, E 521-96, Annual Book of ASTM Standards, Vol 12.02, American Society for Testing Materials, Philadelphia, 1996, 1-20.

11. M. S. Wechsler et al., "Calculation of displacement, gas, and transmutation production in stainless steel irradiated with spallation neutrons," *Journal of Nuclear Materials* **212–215** (1994) 1678–1681.

12. M. S. Wechsler et al., "Radiation Effects in Materials for Accelerator-Driven Neutron Technologies," to be published in *Journal of Nuclear Materials*.

13. M. S. Wechsler, C. Lin, and W. F. Sommer, "Basic Aspects of Spallation Radiation Damage to Materials," *Proceedings of the International Conference on Accelerator-Driven Transmutation Technologies and Applications*, Las Vegas, NV, July, 1994 (AIP Conference Proceedings **346**, 1995) 466–475.

14. M. S. Wechsler, et al., "Calculations of Radiation Damage in Target, Container, and Window Materials for Spallation Neutron Sources," to be published in *Proceedings of the Second International Conference on Accelerator-Driven Transmutation Technologies and Applications*, Kalmar, Sweden, June, 1996.

15. M. S. Wechsler, et al., "Calculation of displacement and helium production at the LAMPF irradiation facility," *Effects of Radiation on Materials: Twelfth International Symposium*, STP 870, ed. F. A. Garner and J. S. Perrin, (Philadelphia, PA: American Society for Testing and Materials, 1985), 1189-1198.

16. L. R. Greenwood and R. K. Smither, "SPECTER: Neutron Damage Calculations for Materials Irradiations" (Report ANL/FPP/TM-197, Argonne National Laboratory, 1985).

17. Y. N. Schubin et al., "Nuclear Data in Accelerator Driven Transmutation Problem," to be published in *Proceedings of the Second International Conference on Accelerator-Driven Transmutation Technologies and Applications*, Kalmar, Sweden, June, 1996.